NASA Technical Memorandum 83617

Vortex Generating Flow Passage Design For Increased Film-Cooling Effectiveness and Surface Coverage

S. Stephen Papell
Lewis Research Center
Cleveland, Ohio

Prepared for the
Twenty-second National Heat Transfer Conference
cosponsored by the ASME and the AIChE
Niagara Falls, New York, August 5–8, 1984

NASA

VORTEX GENERATING FLOW PASSAGE DESIGN FOR INCREASED FILM-COOLING EFFECTIVENESS AND SURFACE COVERAGE

S. Stephen Papell
National Aeronautics and Space Administration
Lewis Research Center
Cleveland, Ohio 44135

ABSTRACT

The present study examines the fluid mechanics of the basic discrete hole film cooling process described herein as an inclined jet in crossflow and hypothesizes a cusp shaped coolant flow channel contour that increases the efficiency of the film cooling process. The design concept requires the channel to generate a counter rotating vortex pair secondary flow within the jet stream by virtue of flow passage geometry. The interaction of the vortex structures generated by both geometry and crossflow was examined in terms of film cooling effectiveness and surface coverage. Comparative data obtained with this new vortex generating coolant passage showed increases up to factors of four in both effectiveness and surface coverage over that obtained with a standard round cross section flow passage. A streakline flow visualization technique was used to support the concept of the counter rotating vortex pair generating capability of the flow passage design.

NOMENCLATURE

A	area
c	centrifugal force
D	drag
d	coolant passage diameter
M	blowing rate $(\rho V)_c/(\rho V)_\infty$
m	momentum change
R	radius
T	temperature
t	adiabatic plate thickness
u	crossflow velocity (tunnel)
V	velocity
x	distance from downstream edge of coolant exit port
x/d	dimensionless distance based on effective hole diameter
η	adiabatic film cooling effectiveness $(T_\infty - T_{aw})/(T_\infty - T_c)$
ρ	density

Subscripts:

aw	adiabatic wall
c	coolant
j	jet
∞	tunnel air, crossflow, or free-stream

INTRODUCTION

Film cooling is well-established as a viable method for protecting turbine blades and vanes in high performance engines for advanced aircraft. Since the coolant itself is drawn from compressor pressurized air that is part of the aerodynamic cycle of the engine, it becomes necessary to use it as efficiently as possible.

In actual use, the coolant enters the base of the blading and is ejected through holes drilled at some angle through the blading walls. Although the coolant passages are generally straight with circular cross section, as for example reported in Ref. 1, some attempts have been made to increase the effectiveness of the film cooling process by design modifications. A survey article by Goldstein (2) describes film cooling geometries tested from slots to round holes. It is also known that engine manufacturing companies are developing inlet and exit passage contouring techniques with encouraging results. The influence of coolant passage curvature on film cooling efficiency was examined in Refs. 3 and 4. It was reported therein that passage curvature increased the effectiveness of the film cooling process by a maximum of about 35 percent at low blowing rates, but at higher blowing rates a trend reversal in the data showed a decrease in effectiveness.

The present study uses an inclined jet in crossflow as a model to hypothesize a coolant channel cross section contour that should increase the effectiveness of the film cooling process. The design concept requires the coolant channel to generate a counter rotating vortex pair secondary flow within the coolant jet by virtue of the shape of the flow channel. The interaction of the vortex structure generated by the coolant passage and the vortex structure generated by

the crossflow was examined in terms of film cooling effectiveness and surface area coverage. Comparative data obtained with a round hole cross section coolant passage were used to evaluate the worth of this new design concept.

Reported herein are the thermal film cooling footprints obtained by infrared imagery for the vortex generating cross section and the round cross section coolant passages embedded at an angle of 30° in adiabatic test plates. The crossflow covered a range of velocities from V_∞ = 15.5 to 45.0 meters per second with blowing rates from M = 0.20 to 2.05. Temperature difference between coolant and crossflow was about 22° C.

FLUID DYNAMIC MODELING

Inclined Jet in Crossflow

The film cooling mechanism is the injection of a cool film of air into a boundary layer to provide an insulating layer between a hot gas and metal surfaces. For the protection of turbine blading the coolant is ejected through discrete holes drilled at some angle in the blade wall so that the basic fluid dynamic process is essentially an inclined jet in crossflow. The literature, as for example Refs. 5 and 6, going back many years contains many studies relating to the mixing process associated with a jet in crossflow.

Figure 1 is a schematic of an inclined jet in crossflow showing the forces on a control element of the jet. The drag (D) acts opposite to the direction of the relative velocity caused by the interaction of the crossflow velocity (V_∞) and the jet velocity V_c. The centrifugal force (C) is normal to the jet path while the momentum change (m) acts along the jet path.

There are three well defined turbulent mixing processes associated with this momentum change that contribute to the breakup of the jet. The first is the mixing that occurs along the interface between the jet and the crossflow. The second is just downstream of the jet exit port where a pressure rarefaction pulls the tunnel air sideways under and into the jet stream. The third mixing process occurs within the jet stream itself with the formation of a vortex structure schematically illustrated in Fig. 2 as a counter rotating vortex pair. The vortex strength and the distance between vortex centers that influences the width of the jet are also influenced by the crossflow momentum. The cross section of the jet (fig. 2) shows that the direction of rotation for this vortex pair structure is down on the sides and up through the center. This direction of rotation, induced by the crossflow is quite significant and will be further discussed in this report.

From this simple model it is evident that the discrete hole film cooling process is controlled by the energy available in the crossflow. It is suggested that this energy is distributed in a manner to influence the jet trajectory, the three turbulent mixing processes described above and the spreading of the jet on the surface to be protected.

The design concept was to modify the coolant jet stream by inducing a vortex structure within the coolant flow, similar to that shown on Fig. 2 by virtue of a unique shaping of the coolant passage. Provided this were possible, it was postulated that this geometrically induced vorticity could replace the crossflow energy required to generate the vortex flow structure within the jet. As a result it was suggested that more crossflow energy would be available to turn the jet closer to the wall and/or increase the vortex strength to spread the jet. Both of these flow mechanisms should increase the effectiveness of the film cooling process.

It was also suggested that the direction of rotation of the counter rotating vortex structure generated by the passage geometry could be reversed with respect to the crossflow generated vortex structure. In this manner both vortex structures would tend to cancel each other out at the coolant port exit. If this were possible, the mixing that occurs due to the tunnel air being pulled sideways and under the jet stream could be prevented or minimized.

Coolant Passage Design Concept

The vortex generating coolant flow passage design concept is illustrated in Fig. 3 along with a standard round hole cross section passage for comparative purposes. The cross section of the vortex generating passage in Fig. 3(a) is somewhat elliptical in shape with a flat surface on one of the long ends of the ellipse and a cusped surface on the opposite end. Figure 3(b) shows the edge of cusp extending along the length of the flow passage that provides the vortex generating capability of the coolant passage.

The double curved surfaces of the cusp should split the flow into two streams that rotate in opposite directions producing a vortex pair structure within the coolant stream. Within the passage the direction of this vortex pair rotation is from the center of the flat surface (fig. 3(a)) toward the cusp edge and out along the curved surfaces in opposite directions. The direction of this geometrically induced rotation with respect to the crossflow, therefore, depends on the orientation of the cusp edge in the flow passage. Figure 4 illustrates two different cusp orientations used in this study. With the cusp surface on the top of the jet stream (fig. 4(a)) the direction of rotation is upward toward the cusp edge and down on the sides. With the cusp surface at the bottom of the jet stream (fig. 4(b)) the rotation is downward toward the cusp edge and upward along the sides.

It therefore follows from Fig. 4 that the vortex structure generated by the top cusp geometry enhances the vortex structure generated by the crossflow by rotating in the same direction while for the bottom cusp geometry both sets of vortex pairs rotate in opposite directions and tend to cancel each other out. The interactions of these sets of vortex pairs and their influence on film cooling efficiency is the subject of this study.

APPARATUS

The actual coolant passage design used for this study is illustrated in Fig. 5 showing the dimensions of the coolant passages. Both the round and vortex generating passages were cast in epoxy as inserts to be installed in the flat plate shown in Fig. 6. The round cross section passage had a flow diameter of 1.27 cm while the countoured vortex generating passage was sized to have the same flow area. In this manner, for the same mass flow, the discharge velocity of the coolant was the same. Both passages discharged the coolant at an angle of 30° with respect to the surface in line with the tunnel flow.

The test plate was made of mahogany with a thickness of 6.35 cm that minimized heat transfer through its wall. In addition, the thick plate also provided a ratio of thickness to coolant passage effective diameter (t/d) equal to 5, which is typical of holes drilled in the walls of cooled turbine blading. The coolant passage inserts were hand-fitted to an opening

in the test plate designed to accept them. The surfaces of the plate and the passage inserts were finished smooth and painted a uniform dull black to increase their radiation emissivity. The top of the plenum (fig. 6) was attached to the bottom of the test plate. The coolant air, supplied to the plenum entered the coolant passage at very low velocity. The plenum assembly contained a system of baffles and screens and was covered with fiberglass insulation.

The test plate and plenum assembly were installed as part of the tunnel floor shown in Fig. 7. The tunnel itself, designed for flow visualization, was made of clear plastic sections with a flow area cross section of 15 cm x 38 cm. A contoured inlet and a transition piece, connected to the altitude exhaust system of the laboratory, completed the tunnel assembly.

The tunnel section containing the test plate was positioned so that there was about 1.3 m of tunnel length (not including the contoured inlet) in front of the coolant injection exit port. In a previous investigation (4) velocity profiles were obtained in this tunnel by both hot-wire and pivot tube probes. These measurements assured the establishment of well-developed turbulent boundary layer at the coolant injection port. Under the flow conditions of this study, the tunnel flow boundary layer thickness was about 1.65 cm and the turbulence intensity of the free-stream was about 3 percent.

The coolant was supplied to the plenum by use of a Hilsch tube connected to a 120 psi dry air source. This source, which incorporates a vortex generator element, separates the inlet air into hot and cold streams. This results from the forced vortex or wheel type of angular velocity imparted to the air entering the device. Conservation of total energy of the inner portion of the contained vortex causes heat to be transferred to the outer region of the vortex. Consequently, a relatively cold inner core of air and a warm outer ring of air are available. In the Hilsch tube design the warm and cold air discharge ports are on opposite ends of the tube. Cold side temperatures of 0° C are available with this device so that temperature differences between the tunnel and coolant air flow of about 22° C could be readily obtained.

The tunnel air temperature was measured with a thermocouple mounted in the contoured inlet. The coolant air temperature was measured with a thermocouple mounted in the plenum between the screens and the mahogany test plate. The coolant airflow rate was measured with a turbine type flowmeter installed between the Hilsch tube and the coolant plenum.

The infrared camera and detector unit used to measure the surface temperature downstream of the coolant injection port was capable of operating within the temperature range of -30° to 200° C and could discriminate temperature differences as small as 0.2° C. The detector element was indium antinomide cooled by a liquid nitrogen bath. The detector displayed the isotherm image on the cathode-ray screen, from which it was then photographed for a permanent record. A reference isotherm at a known temperature was obtained for each data run by focusing the camera on the test plate at a position not influenced by the cooling air jet. The temperature at this position was measured with thermocouples embedded in the plate.

Examples of photographic data are shown in Fig. 8 which presents equal temperature isotherm trace comparison between the round and cusped coolant channels for data obtained at identical test conditions. The temperatures of the isotherm traces are indicated in thermal scale units by the tick marks along the abscissa on the photographs. The comparison between these scale readings and the reference scale readings previously described permit the evaluation of the isotherm temperatures. The two vertical lines on the photographs are the field-of-view limits of the infrared detector. These lines are centered so that the left line butts up to the downstream edge of the coolant injection part which is not displayed on the photograph.

Experimental Procedure and Data Reduction

The experimental data obtained for this study enabled the evaluation of film cooling effectiveness and surface area coverage for each isotherm trace. The controlled parameters for these tests were tunnel air velocity (crossflow), coolant velocity, and coolant temperature. The coolant temperature, measured in the plenum, was set near 0° C by controlling the Hilsch tube valves. The tunnel air temperature, depending on ambient conditions, was about 25° C. Variations in the blowing rate were obtained by control of tunnel and Hilsch tube airflow valve settings.

The testing procedure required an initial cool down of the plenum before a desired blowing rate was set. The temperatures were then allowed to come to equilibrium before data collection commenced. A series of 8 infrared photographs were obtained for each test setting that covered the temperature range of the film cooling footprint. The testing procedure was repeated over a range of tunnel velocity settings and blowing rates for data obtained with the standard round hole cross section coolant passage and the top cusp and bottom cusp orientations of the new vortex generating coolant passage.

The film cooling effectiveness of each isotherm trace was calculated as:

$$\eta = \frac{T_\infty - T_{aw}}{T_\infty - T_c} \qquad (1)$$

where T_∞, T_c, and T_{aw} are temperatures of the tunnel air, coolant and plate, respectively. Information gained from these traces also included interpretations of isotherm shapes with regard to the mixing processes of both air streams. For example, the photographs in Fig. 8 pictorially illustrate differences in equal temperature isotherm traces obtained under the same test conditions for the round and top cusp coolant passage geometries. Differences in size and shape of the traces are readily observed. The round hole trace in Fig. 8(a) closes on itself at the end nearer to the coolant exit port. Since the plate surface temperature outside of the enclosed trace is warmer than the trace itself, the warmer plate temperature near the coolant exit port suggests that the jet did not attach to the surface until some distance downstream. The pressure rarefaction that occurs just downstream of the exit port due to the passage angularity with respect to the tunnel flow is responsible for this flow separation phenomena.

Two types of measurements were obtained from the infrared photographs. The first was the centerline length of each isotherm trace measured from the downstream edge of the coolant injection port to the downstream edge of the trace. The second measurement, performed with a planimeter, was the surface area enclosed by the trace. The results of this investigation, presented graphically, covered data obtained at specific test conditions of tunnel velocity V_∞ = 15.5, 22.8, 30.5, and 45.0 m/s and blowing rates from M = 0.20 to 2.05 for each of the three coolant passage geometries.

PRESENTATION OF DATA AND FLOW PHENOMENA

Examples of Data Plots

Figure 9 is presented as an example of data obtained at a tunnel velocity of V_∞ = 22.5 m/s and blowing rate of M = 1.25. Difference in the level of the curves for the three coolant passage configurations are readily apparent. The centerline film cooling effectiveness plotted in Fig. 9(a) as a function of dimensionless distance (x/d) illustrates the inferior performance of the standard round hole coolant flow passage. The top cusp passage is superior for x/d distances greater than approximately 3 but near the injection port the bottom cusp passage is best. An examination of Fig. 9(a) shows a factor of four difference between the round and the bottom cusp data just downstream of the coolant exit port.

The film cooling coverage data in Fig. 9(b) shows a more regular trend than that of the effectiveness data. The round passage data again show the inferior performance of the standard passage compared to either cusp orientation of the vortex generating passage. The top cusp passage is the best with the bottom cusp data falling in between but closer to the top cusp curves. An examination of Fig. 9(b) shows that for a constant effectiveness value of 0.15 there is about a factor of four increase in surface area coverage between the round and the top cusp data.

The individual data points, through which the curves were drawn, are included in Fig. 9 to illustrate the extent of scatter which is typical of all the data obtained for this study. For the remaining figures in this report only the curves themselves will be presented.

Trends in Centerline Effectiveness

The film cooling effectiveness data trends as a function of blowing rate from M = 0.20 to M = 2.05 are illustrated in Fig. 10. Although this set of data was obtained at a tunnel velocity of V_∞ = 15.5 m/s, the data trends that appear herein are quite similar for tunnel velocities up to and including V_∞ = 45.0 m/s. Each set of figures, at a constant value of blowing rate, is a plot of effectiveness as a function of dimensionless distance (x/d). The solid lines represent the round hole data while the dashed and the broken lines represent the top cusp and the bottom cusp data, respectively.

At all blowing rates the film cooling performance of the standard round cross section passage is inferior to the new vortex generating passage in either cusp orientation. For dimensionless distances (x/d) greater than four the data trends are quite regular. The top cusp data shows the highest film cooling effectiveness while the round hole data shows the lowest effectiveness. The bottom cusp data falls in between with its position relative to the top cusp and round hole data a function of blowing rate. At low blowing rates the bottom cusp data falls close to the round hole data but shifts in the direction closer to the top cusp data as the blowing rate is increased.

For dimensionless distance (x/d) less than four which is close to the coolant exit port, a reversal occurs in the relationship between both cusp orientations of the vortex generating passage with the bottom cusp passage becoming more effective. The effectiveness difference increases considerably as the blowing rates are increased.

The general conclusion drawn from the data in Fig. 10 is that the top cusp coolant passage is superior in effectiveness to both the bottom cusp and the round hole passage except close to the coolant exit port where at blowing rates equal to and greater than M = 1.00, the bottom cusp passage becomes superior. Differences in film cooling effectiveness up to factors of four (fig. 10(e)) can be obtained by choice of coolant passage geometry.

Trends in Film Cooling Coverage Data

Trends in the film cooling coverage data as a function of blowing rate for data obtained at a tunnel velocity of V_∞ = 15.5 m/s are illustrated in Fig. 11. Each set of curves, for a constant value of blowing rate, presents film cooling effectiveness in terms of isotherm area coverage. The solid lines represent the round hole data while the dashed lines and the broken lines represent the top cusp and the bottom cusp data, respectively.

Data trends illustrated in Fig. 11 show the superior performance of the top cusp passage over the round passage for the entire range of blowing rates from M = 0.20 to M = 2.05. The bottom cusp data lie between these two sets of curves in a position that depends on the blowing rate. At the lowest blowing rate of M = 0.20 (fig. 11(a)) the bottom cusp data plots on or close to the round passage curves. With increasing blowing rate the bottom cusp curves shift in the direction of the top cusp curves and at M = 2.05, both curves almost coincide. These data trends are representative of all the film cooling coverage data obtained for this investigation up to and including tunnel velocities of V_∞ = 45.0 m/s.

In general, it appears that for the same film cooling effectiveness and flow conditions the flow from the top cusp passage covers a larger surface area than is available from the coolant flow from the round hole passage. In addition, the surface area covered by the coolant flow from the bottom cusp passage plots in between at a relative position depending on the blowing rate. Differences in surface area coverage of up to a factor of four (fig. 11(e)), can be attained by choice of coolant passage geometry.

DISCUSSION

The improved film-cooling performance of the vortex generating coolant passage over the standard round cross section passage has been demonstrated herein for the range of blowing rates relevant to turbine blade cooling from M = 0.20 to M = 2.05. The evidence is graphically presented in terms of comparative data plots obtained under identical test conditions. Differences in the data were explained by using an inclined jet in crossflow as a model that led to the concept of a vortex generating coolant passage design. It was determined that the coolant passage, by virtue of its geometry, generates a counter rotating vortex pair structure within the coolant flow that is similar to the vortex structure generated by the crossflow. The cusped surface coolant passage design evolved along the following arguments. Because the cusped surface in the coolant passage controls the vortex pair direction of rotation it was believed that a change in rotation direction could be achieved by orienting the cusped surface on the top or at the bottom of the jet stream. It was also believed that this difference in inducted vortex rotation would influence the data. The vortices generated by the top cusped geometry enhance the vortex structure generated by the crossflow because they rotate in the same direction while for the bottom cusped geometry both sets of vortex pairs rotate in opposite directions and tend to cancel each other out. The fluid dynamic interactions

of these sets of vortex pairs were used to explain the differences in the data.

There are separate arguments that apply to the different orientations of the cusp shaped coolant passage. When the cusp surface in the passage is on top of the jet stream, both geometry and crossflow induced vortex rotations are in the same direction. For this orientation it was hypothesized that when the flow is discharged into the tunnel mainstream the geometrically induced vortices are already present and do not require initiation by the main stream. Consequently, the mainstream has more momentum available to turn the jet closer to the wall resulting in enhanced film cooling effectiveness.

When the cusped surface is oriented on the bottom of the jet stream, both vortex structures rotate in opposite directions and influence the jet separation phenomena previously described. Both the round hole and top cusp coolant passages allow flow separation to occur due to a pressure rarefaction that occurs just downstream of the injection port resulting in a side flow pumping of the tunnel air under and into the jet stream. The direction of vortex pair rotation with the passage in the bottom cusp orientation must therefore be responsible for preventing or minimizing this pumping from occurring.

Although the significant isotherm data difference measurements obtained with the round, top cusp and bottom cusp coolant passages could be attributed to geometry differences, speculation of the counter rotating pair vortex generating capability of the cusp shaped passage could only be hypothetical. Therefore, immediately following the isotherm data collecting phase of this investigation a flow visualization study was initiated to attempt to visually establish the expected vorticity in the flow. A streakline flow visualization technique was used that photographed approximately 1-mm-diameter neutrally buoyant helium filled "soap" bubbles, which are reported in Ref. 7 to follow the flow field. With a camera shutter speed of 12 frames per second the bubble appears as a streakline on the film. The bubble generator outlet probe was set up to discharge into the coolant plenum thereby seeding the coolant flow. The indication of vorticity in the flow is then captured on film and can be identified by the twisting motions of the streaklines.

The set of 3 photographs in Fig. 12 were obtained using a telephoto lens with the camera facing downstream from the tunnel inlet toward the front edge of the test plate. The horizontal white line in these photos is the surface of the test plate illuminated by the lamp that defines the exit end of the coolant passage. In the absence of tunnel crossflow, Fig. 12(a) shows a streakline rising from the the top cusp passage toward the top of the tunnel. The camera caught the bubble streak after it had emerged from the passage. The twisting motion of this streakline suggests that, without crossflow, this vorticity must have been generated by the geometry of the coolant passage.

The photographs in Figs. 12(b) and (c) were obtained under conditions of crossflow with both the top and bottom cusp passages subjected to the same blowing rate of M = 0.34 but at different tunnel flow rates. The crossflow momentum appears to have turned the coolant jet toward the surface away from the camera. The streaklines that appear to be moving into the paper reveal the twisting motion of the jet as it emerges from the edge of the coolant passage indicating vorticity. The counter rotating vorticity in the flow is also supported by these photos because the camera caught the sets of bubbles coming out of the passage at the same time that appear to be rotating in opposite directions. The division of flow in Figs. 12(b) and (c) appears quite clear but unfortunately the sense of rotation direction for the individual streams can only be speculated.

One of the speculations that could be satisfied by photography is the change in trajectory of the jet stream caused by differences in coolant passage geometry. This was accomplished by setting up the camera at the side of the tunnel to photograph the side edge of the test plate. Figure 13 shows a streakline emerging from top cusp passage with no crossflow. The jet flow ejects from the passage at an angle of 30° with respect to the plate surface. The pointer on the transparent wall of the tunnel is located at the downstream edge of the ejection port and establishes a reference measurement position. The bolt through the test plate and the edge of the tunnel wall that appears as a lighted object above the test plate establishes a reference position for obtaining the height of the streamline at a fixed position downstream from the coolant exit port. An examination of Fig. 13 will show that, without crossflow, the vorticity appearing in the streakline could be attributed to the cusp passage geometry. This figure supports the front tunnel view picture (fig. 12(a)) that also shows vorticity generated by the passage geometry.

The change in trajectory of the jet stream caused by differences in passage geometry, under identical flow conditions, is illustrated in the set of photographs in Fig. 14. Using the top of the bolt in the tunnel wall as a reference position it is apparent that the jet trajectory from the round hole passage (fig. 14(a)) is significantly higher than the trajectories from the top and bottom cusped passages shown in Figs. 14(b) and (c). Referring back to Figs. 10(f) and 11(f), that present film cooling data comparisons under the same conditions as these photographs, the inferior film cooling performance of the round jet passage over the top and bottom cusp passages is supported by these differences in trajectory.

SUMMARY OF RESULTS

The film cooling isotherm data reported herein were obtained by infrared photography along with an apparatus designed to determine the film-cooling performance of three types of discrete hole coolant flow passages. The passages were embedded in adiabatic test plates and discharged the flow at an angle of 30° in line with the tunnel flow. One of the coolant passages had a standard round hole cross section which was used as a reference to compare the performance of two orientations of a counter rotating vortex pair generating coolant passage that evolved from an examination of the basic fluid dynamics of an inclined jet in crossflow.

Test conditions included blowing rates from M = 0.20 to 2.05, tunnel velocities from V_∞ = 15.5 to 45.0 m/s, with temperature differences of about 22° C between the tunnel and coolant air streams. Data comparisons are presented graphically as film cooling effectiveness in terms of the centerline length of the isotherm traces measured from the edge of the coolant injection port and also the surface area enclosed by the isotherm.

Interactions of the vortex pair structure in the coolant flow generated by passage geometry with the vortex pair generated by the crossflow was found to influence the film cooling process. Comparative data obtained under the same test conditions showed up to factors of 4 increases in both centerline film cooling effectiveness and surface area coverage over that obtained with a standard round cross section passage.

In addition, it was determined that flow separation of an inclined jet from the surface containing the passage could be depressed by coolant passage geometry that generates a counter rotating vortex pair structure in the coolant flow that rotates in opposition to the crossflow generated vortex pair rotation.

A streakline flow visualization technique was used to support the concept of the counter rotating capability of the cusp faced flow passage design. Photographic data showed the coolant flow split into two streams that rotate in opposite directions. In addition, the streakline trajectory from the round passage was considerably higher than from either the top cusp or bottom cusp passages attesting to differences obtained in the film cooling data.

REFERENCES

1. Goldstein, R. V.; Eckert, E. R. G.; and Ramsey, J. W.: "Film Cooling with Injection Through a Circular Hole", HTL-TR-82, Minnesota Univ., NAS3-7904; NASA CR-54604, 1968.
2. Goldstein, R. V.: "Film Cooling," Advances in Heat Transfer, Vol. 7, T. F. Irvine, Jr. and J. P. Hartnett, eds., Academic Press, New York, 1971, pp. 321-379.
3. Papell, S. S., Graham, R. W., and Cageao, R. P., "Influence of Coolant Tube Curvature on Film Cooling Effectiveness as Detected by Infrared Imagery," NASA TP-1546, 1979.
4. Papell, S. S., Wang, C. R., and Graham, R. W., "Film-Cooling Effectiveness With Developing Coolant Flow Through Straight and Curved Tubular Passages," NASA TP-2062, 1982.
5. Abramovich, G. N., The Theory of Turbulent Jets, M.I.T. Press, Cambridge, 1963.
6. Keffer, J. F., and Baines, W. D., "The Round Turbulent Jet in a Cross-Wind," Journal of Fluid Mechanics, Vol. 15, No. 4, Apr. 1963, pp. 481-496.
7. Colladay, R. S., and Russell, L. M., "Streakline Flow Visualization of Discrete-Hole Film Cooling With Normal, Slanted, and Compound Angle Injection," NASA TN D-8248, 1976.

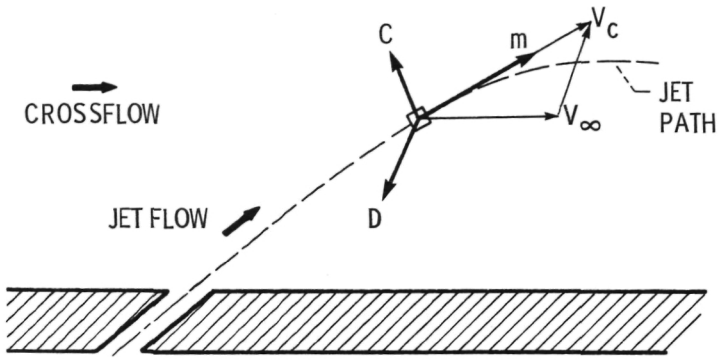

Figure 1. - Schematic of an inclined jet in crossflow showing forces on a control element: D = drag, C = centrifugal force, m = momentum change.

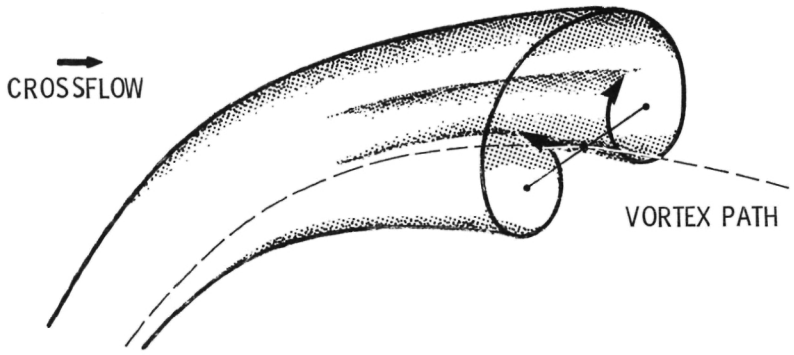

Figure 2. - Schematic of a counter rotating vortex pair structure within the jet induced by the crossflow.

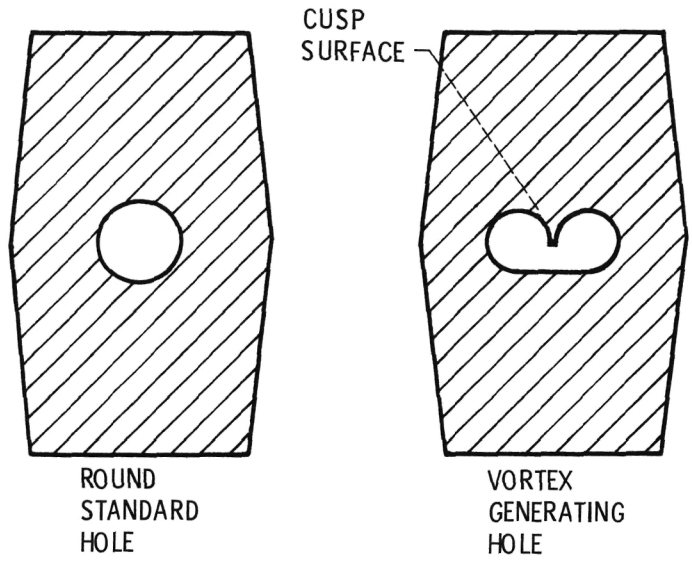

(a) Coolant flow passage cross sections.

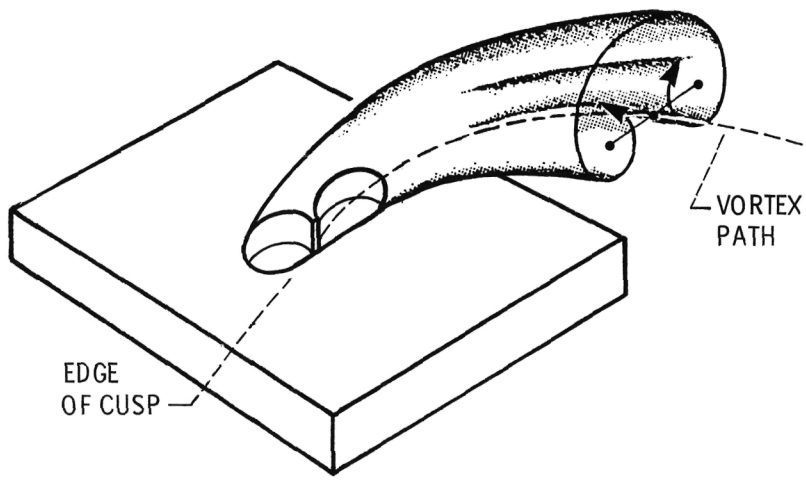

(b) Counter rotating vortex generating coolant passage.

Figure 3. - Design concept.

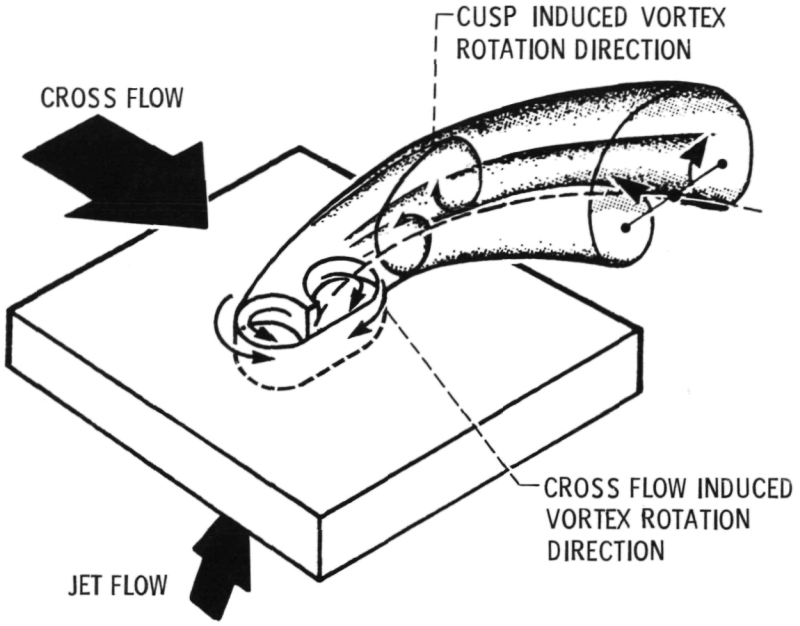

(a) Top cusp.

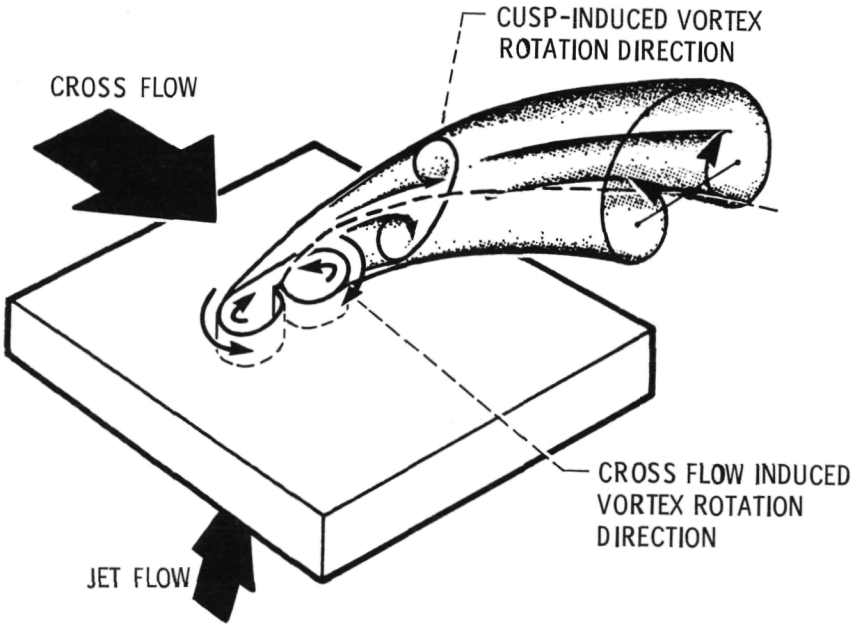

(b) Bottom cusp.

Figure 4. - Geometry oriented cusp induced rotation of vortex pairs with respect to cross flow induced vortex rotation.

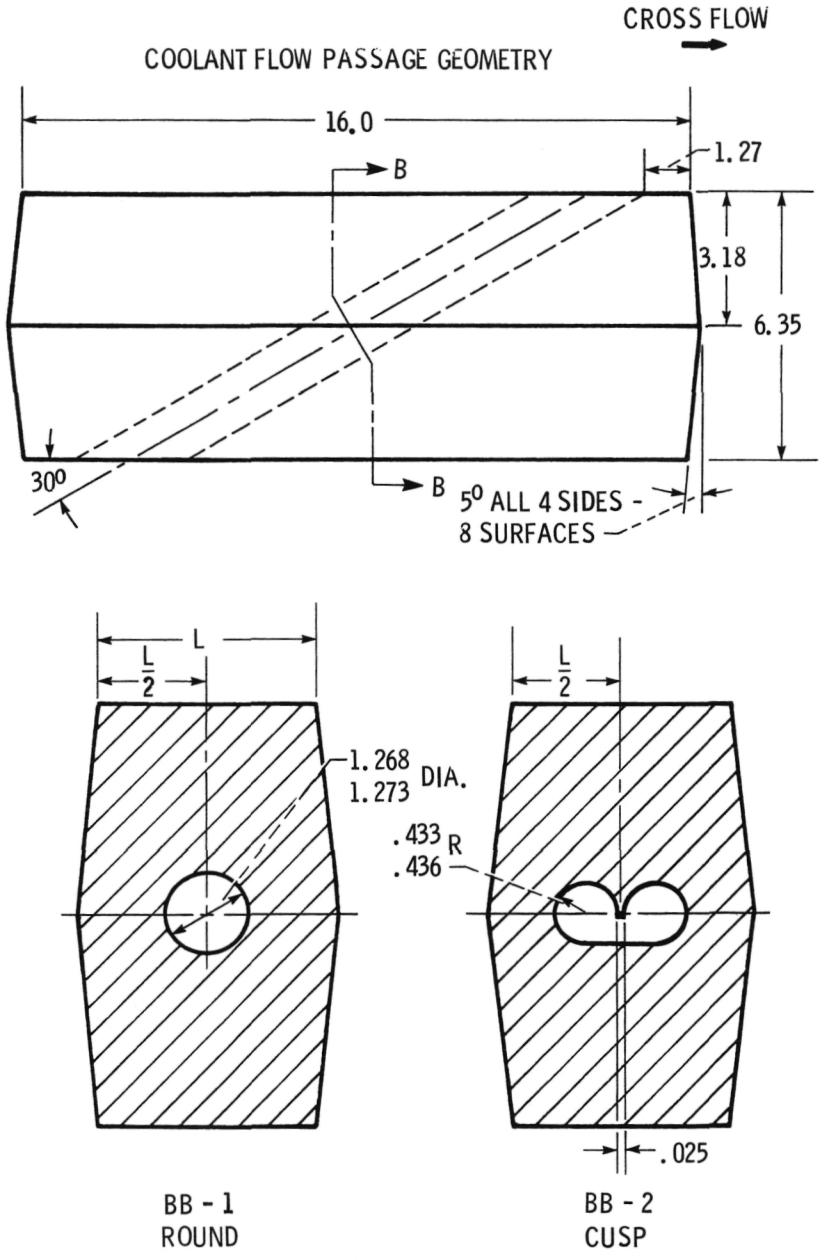

Figure 5 - Actual design of both passage cross sections with equal flow areas. (all dimensions, cm)

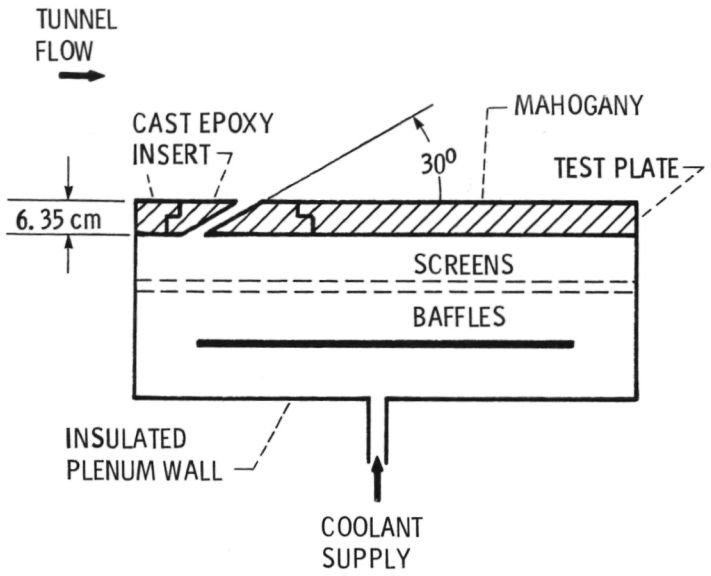

Figure 6. - Schematic of test plate and coolant supply plenum.

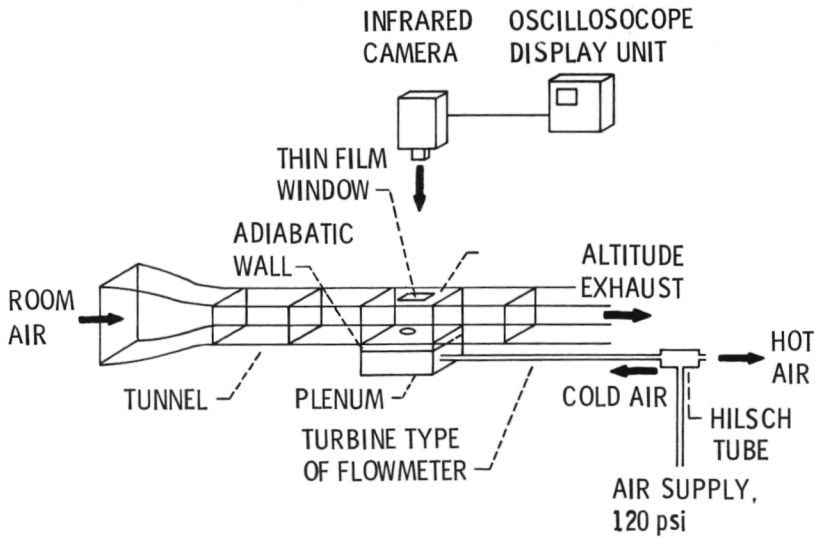

Figure 7. - Schematic drawing of film-cooling rig.

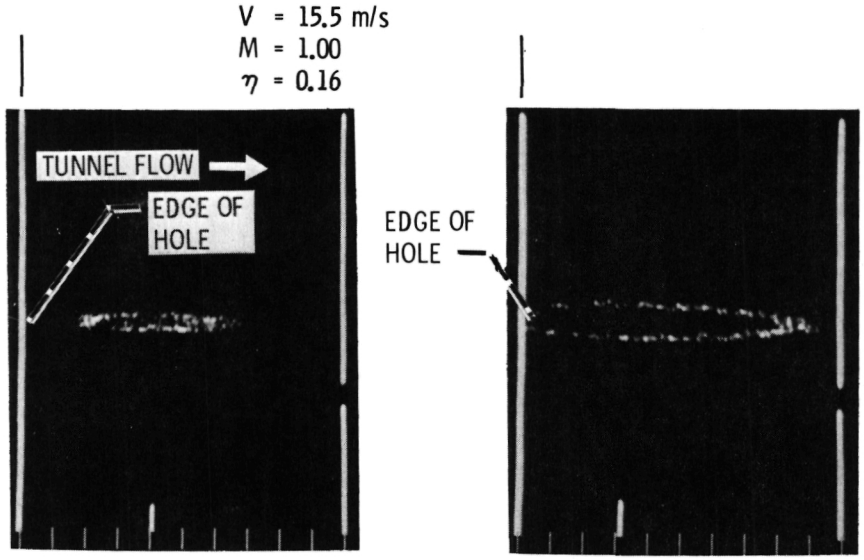

(a) Round. (b) Cusp on top.

Figure 8. - Examples of equal temperature isotherm traces. Infrared photographs obtained under same test conditions.

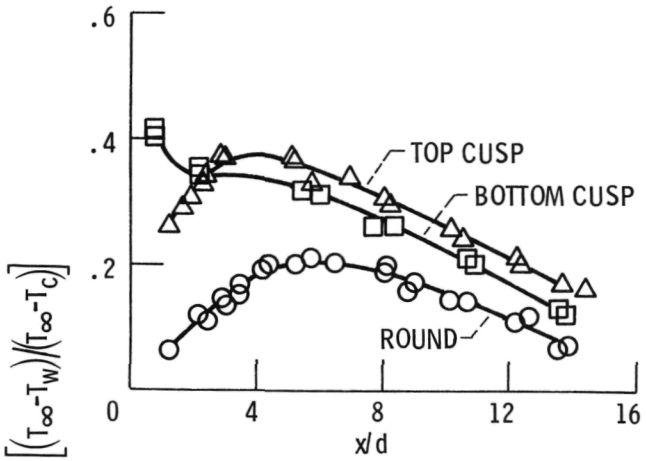

(a) Centerline film cooling effectiveness.

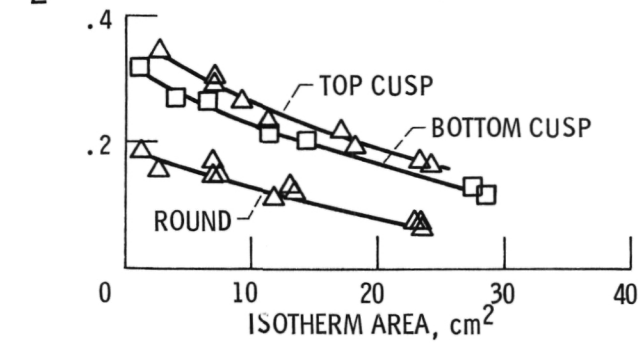

(b) Film cooling coverage.

Figure 9. - Examples of film-cooling data obtained with round, top cusp and bottom cusp coolant passages: V_∞ = 22.5 m/sec; M = 1.25.

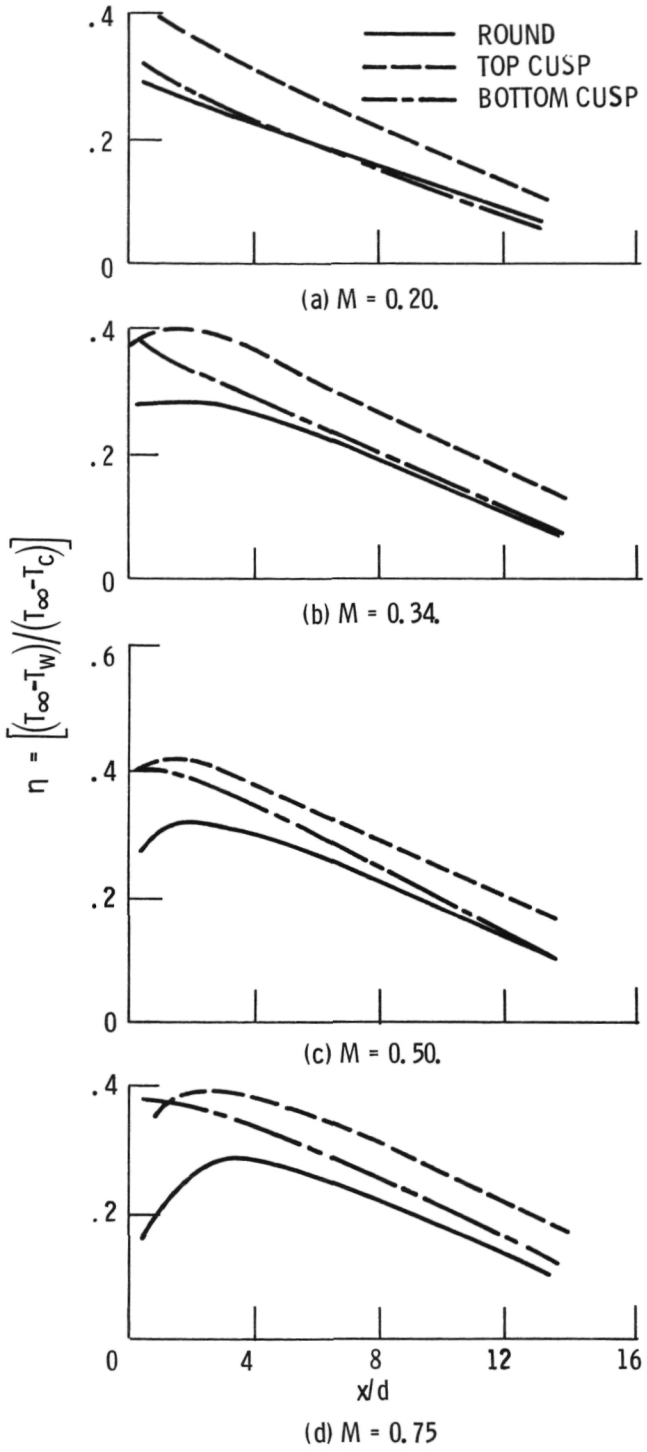

Figure 10. - Comparative data of centerline film-cooling effectiveness distributions for round, top cusp, and bottom cusp passages; 30^0 injection angle; V_∞ = 15.5 m/sec; M = 0.20 to 2.05.

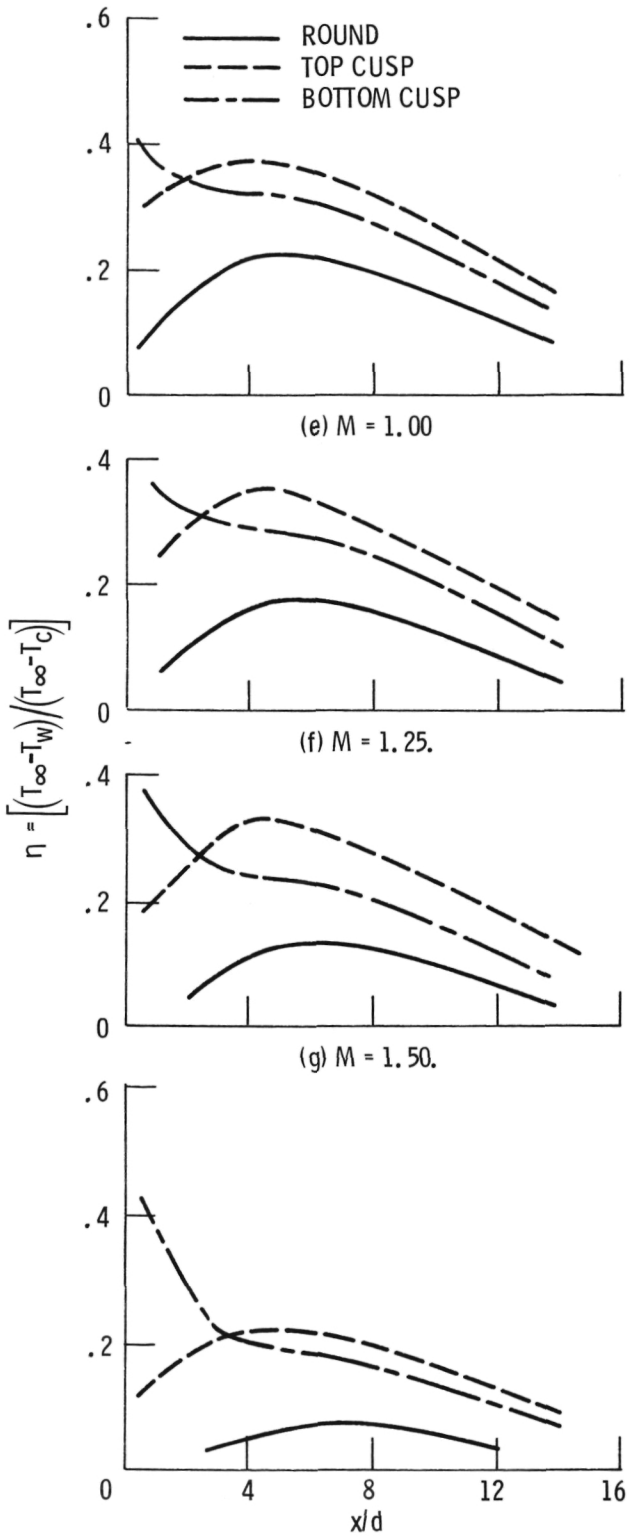

(e) M = 1.00

(f) M = 1.25.

(g) M = 1.50.

(h) M = 2.05.

Figure 10. - Concluded.

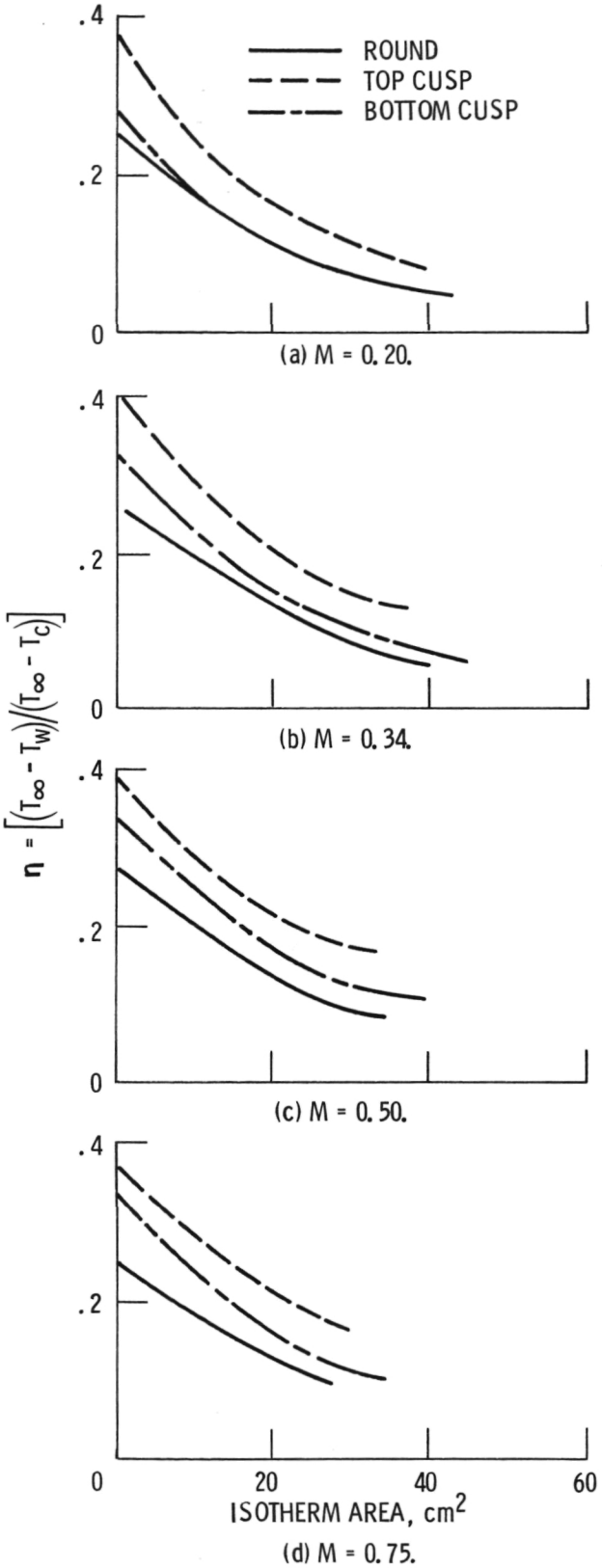

Figure 11. - Film-cooling effectiveness as a function of isotherm area for round, top cusp, and bottom cusp passages; 30^0 injection angle; V_∞ = 15.5 m/sec; M = 0.20 to 2.05.

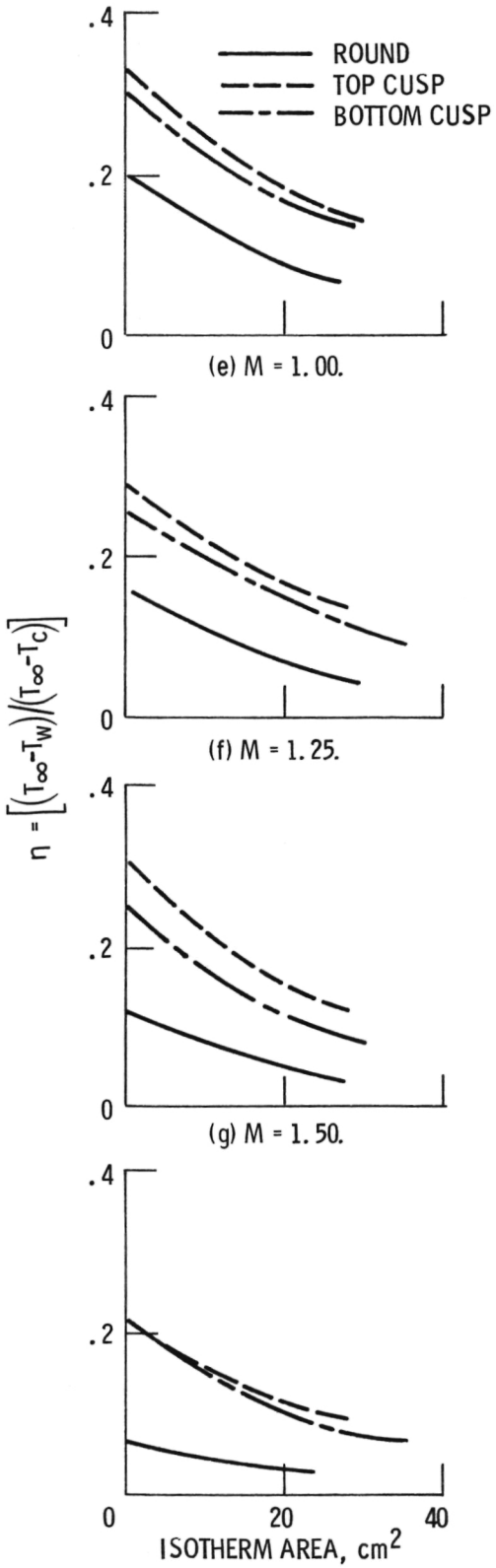

(e) M = 1.00.

(f) M = 1.25.

(g) M = 1.50.

(h) M = 2.05.

Figure 11. - Concluded.

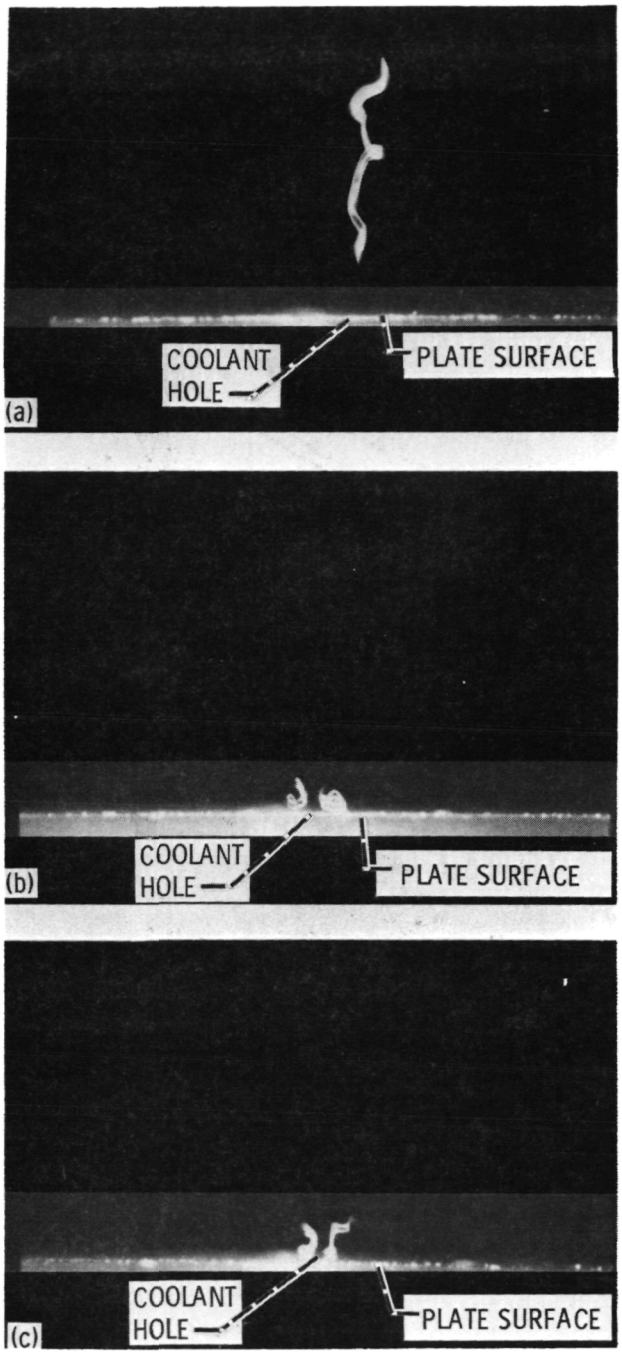

Figure 12. - Tunnel view looking downstream.

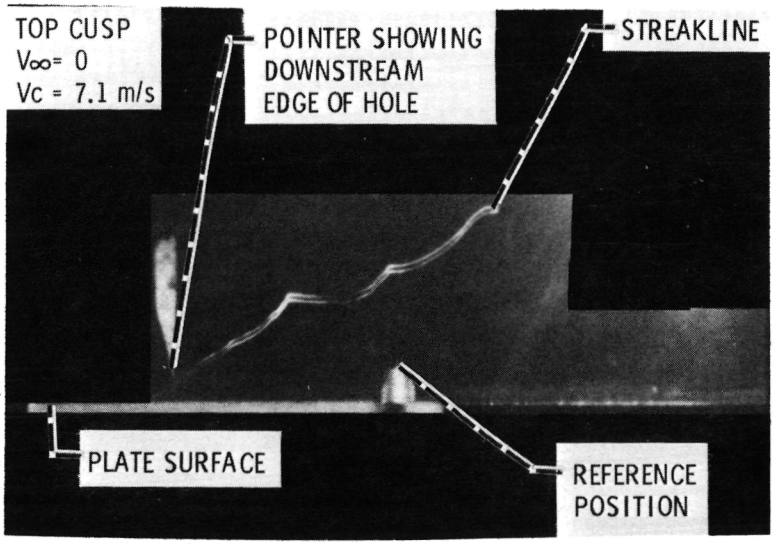

Figure 13. - Side view.

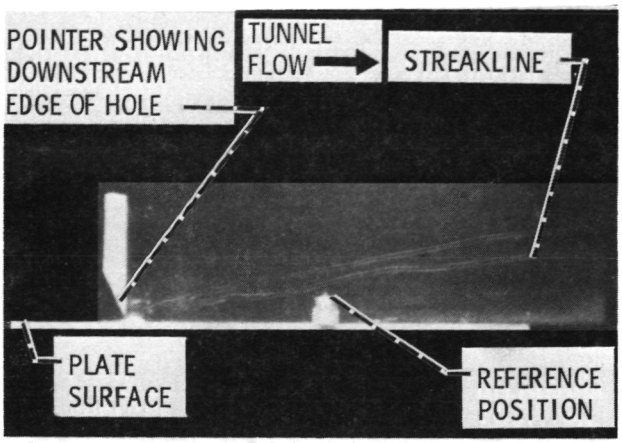

(a) Round.

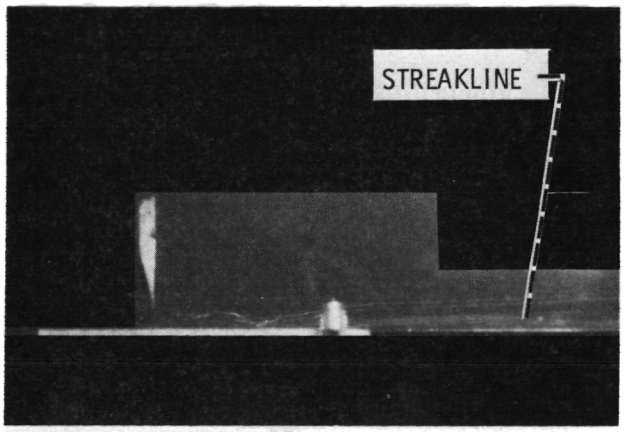

(b) Top cusp.

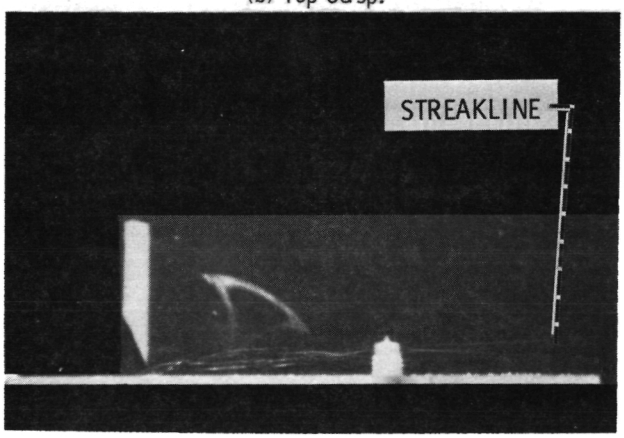

(c) Bottom cusp.

Figure 14. - Side view. V_∞= 15.2 m/s; Vc = 18.7 m/s; M = 1.25.

1. Report No.	2. Government Accession No.	3. Recipient's Catalog No.
NASA TM-83617		

4. Title and Subtitle	5. Report Date
Vortex Generating Flow Passage Design For Increased Film-Cooling Effectiveness and Surface Coverage	6. Performing Organization Code 505-31-42

7. Author(s)	8. Performing Organization Report No.
S. Stephen Papell	E-2048
	10. Work Unit No.

9. Performing Organization Name and Address	11. Contract or Grant No.
National Aeronautics and Space Administration Lewis Research Center Cleveland, Ohio 44135	13. Type of Report and Period Covered Technical Memorandum
12. Sponsoring Agency Name and Address	14. Sponsoring Agency Code
National Aeronautics and Space Administration Washington, D.C. 20546	

15. Supplementary Notes

Prepared for the Twenty-second National Heat Transfer Conference cosponsored by the ASME and AIChE, Niagara Falls, New York, August 5-8, 1984.

16. Abstract

The present study examines the fluid mechanics of the basic discrete hole film cooling process described herein as an inclined jet in crossflow and hypothesizes a cusp shaped coolant flow channel contour that increases the efficiency of the film cooling process. The design concept requires the channel to generate a counter rotating vortex pair secondary flow within the jet stream by virtue of flow passage geometry. The interaction of the vortex structures generated by both geometry and crossflow was examined in terms of film cooling effectiveness and surface coverage. Comparative data obtained with this new vortex generating coolant passage showed up to factors of four increases in both effectiveness and surface coverage over that obtained with a standard round cross section flow passage. A streakline flow visualization technique was used to support the concept of the counter rotating vortex pair generating capability of the flow passage design.

17. Key Words (Suggested by Author(s))	18. Distribution Statement
Film cooling Vorticity Design Coolant passage	Unclassified - unlimited STAR Category 34

19. Security Classif. (of this report)	20. Security Classif. (of this page)	21. No. of pages	22. Price*
Unclassified	Unclassified		

*For sale by the National Technical Information Service, Springfield, Virginia 22161

National Aeronautics and
Space Administration

Washington, D.C.
20546

Official Business
Penalty for Private Use, $300

SPECIAL FOURTH CLASS MAIL
BOOK

Postage and Fees Paid
National Aeronautics and
Space Administration
NASA-451

NASA

POSTMASTER: If Undeliverable (Section 158
Postal Manual) Do Not Return